

Adopting Dynamic Var Compensators to Mitigate PV Impacts on Unbalanced Distribution Systems – Phase II

Mesut Baran, Hanpyo Lee

Overview

D-VAR is an emerging technology which is designed for distribution level Volt/VAR applications. It is a Feeder-ready shunt power electronics-based VAR compensator that can provide precise& continuous injection of VAR (Q) into the system.

D-VAR offers the following benefits:

- Provides effective mitigation on feeders with High Solar PV for
 - power quality or voltage flicker
 - voltage rise and variation
- Provides effective Volt/VAR compensation

The second phase of the project focuses on development of control methods for the D-VAR such that the benefits of D-VAR offer can be maximized. The need for proper control scheme is highlighted in Phase I as it showed that in order to maximize the benefits of a D-VAR a proper dispatching scheme is needed for the D-VAR. Using the standard Volt-Var characteristic based control may not be the best approach, and this approach may significantly reduce the expected benefits from D-VAR. Hence, in Phase II the focus is on the development of more dynamic dispatching schemes (i.e., Shifted and Fitted Volt/Var Curves) for the D-VAR such that the expected benefits are maximized.

When a large PV farm is connected to a distribution feeder, it increases the voltage variation on the feeder, especially during cloudy days. A Dynamic Var Compensator (DVC), such as D-VAR, offers a good alternative in reducing the voltage variations in such conditions. This is selected as the main benefit of a DVC in this work. Hence, the first task involved determining an optimal dispatching scheme for a DVC in order to minimize the voltage variation on a feeder. This dispatching scheme is then used to determine a proper location to place the DVC in order to maximize its benefits (reducing voltage variation on the feeder). The final goal is to determine a practical dispatching scheme by adjusting the local DVC control which uses the typical Volt/Var-Characteristics (VVar-C).

1. Voltage Variation on a Feeder

The main benefit of utilizing a DVC is the mitigation of voltage variations on a distribution feeder. Voltage variation is directly associated with the degree of voltage fluctuation at each node along the feeder. To maintain voltage variations within the desired limits, typically defined by voltage violation thresholds specified in ANSI standards, utilities employ Line Voltage Regulators (LVRs) and Capacitor Banks (CAPs). The Category I limits, commonly adopted by utilities, range between 0.96 and 1.05 pu. However, with the implementation of Conservation Voltage Reduction (CVR), utilities aim to further reduce voltages on feeders, necessitating tighter control over voltage variations. The DVC proves valuable in achieving this objective by ensuring that voltages remain

within a specific target voltage band. This paper considers a voltage band of 0.98 ~ 1.03 pu, as depicted in Fig. 1.

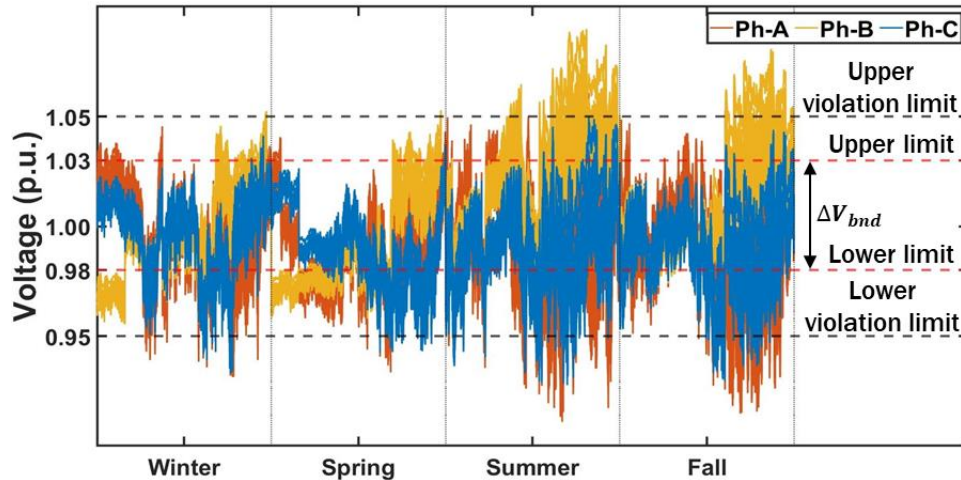


Fig. 1 Voltage variation limits considered for DVC.

2. Optimal DVC Dispatch & Placement

Since DVC injects reactive power, our first observation is that it will affect the voltages mainly in the voltage zone in which it is placed. To illustrate this, consider the sample feeder. Time-series power flow simulations are first conducted on the feeder with no DVC (i.e., base case). On this system the LVR (i.e., 160R) on the main feeder divides the feeder into two voltage zones as indicated on Fig.2: Zone 1 is the first voltage zone (in orange) and Zone 2 is the second zone (in green).

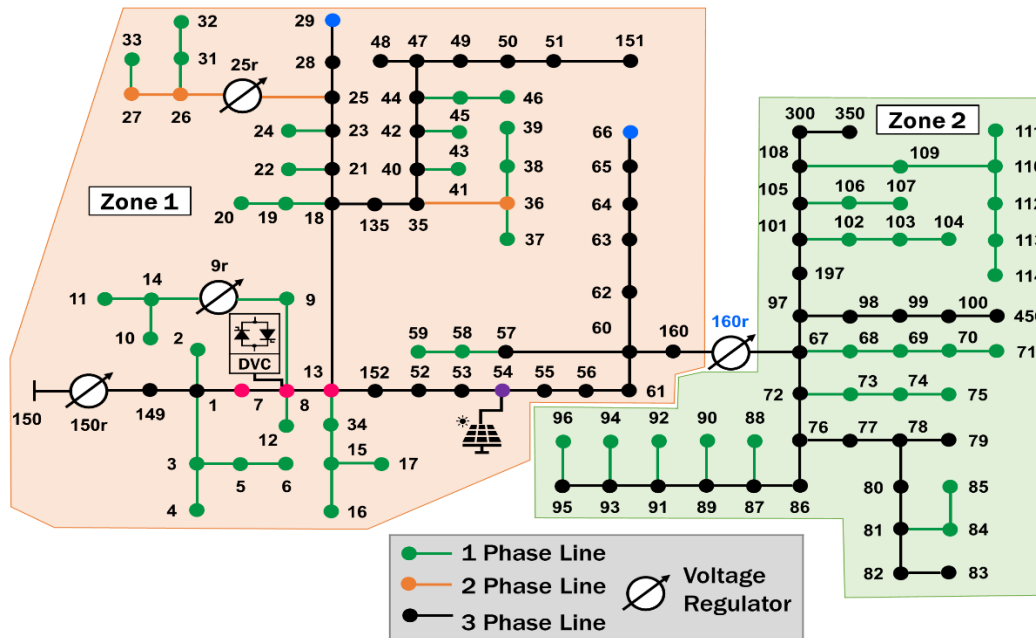


Fig. 2 IEEE 123 test system with high penetration PV and a DVC deployed.

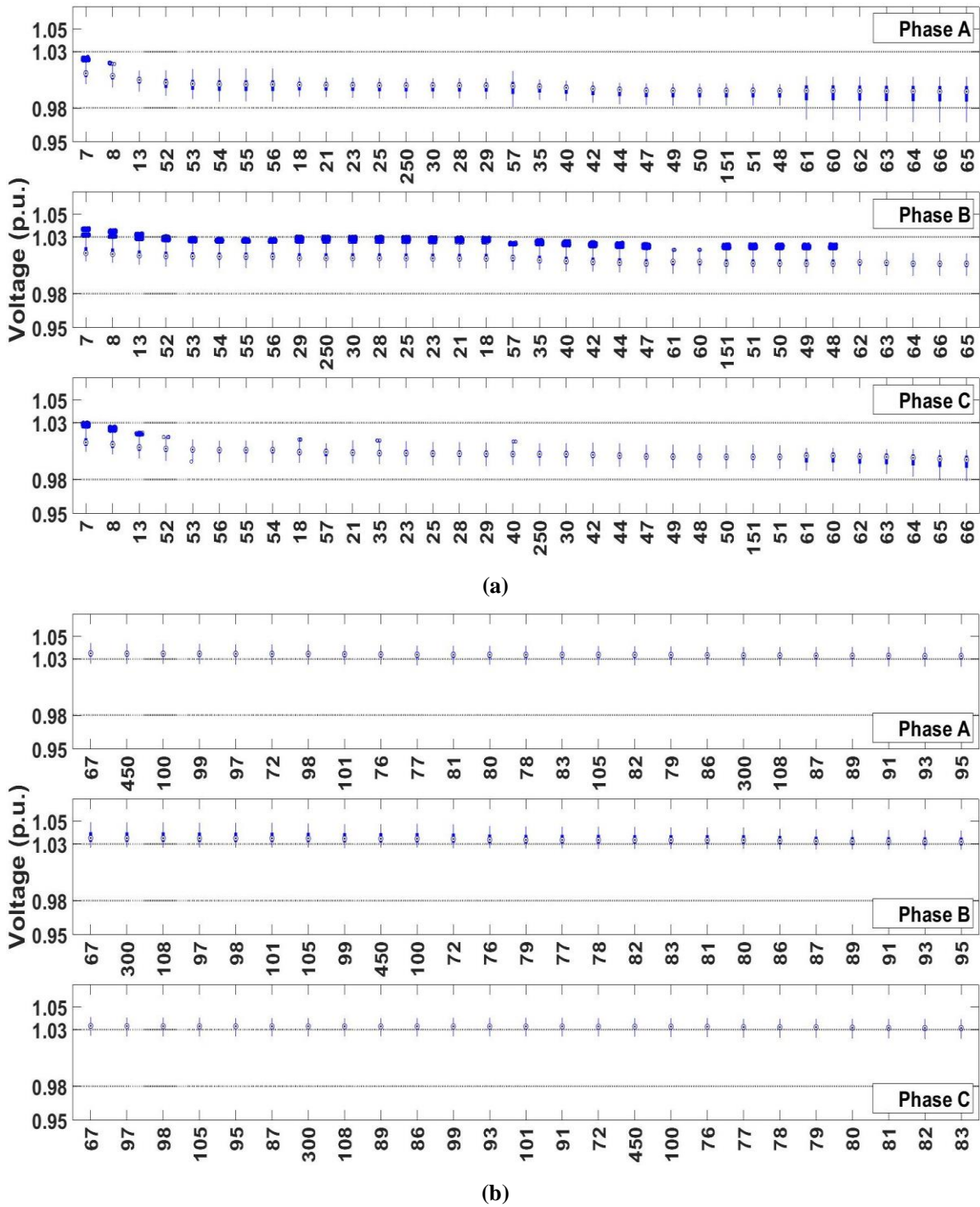


Fig. 3 Node voltage distribution by phase in descending order, (a) Zone 1, (b) Zone 2.

Figure 3 shows the voltage distribution by phase, sorted in descending order by average voltage. The figure illustrates how different the voltage variations are between the two zones. Zone 1 has much larger voltage variation than Zone 2 (and even maximum voltage limit violations) due mainly to large PV farm. Zone 1 has also larger voltage unbalance between phases than Zone 2. Hence, in this case, we want to investigate the effectiveness of the DVR in reducing voltage variations in Zone 1.

2.1 Optimal DVC Dispatch

The dispatching of a DVC entails determining the desired Var injection to be provided by the DVC in order to maintain the voltages on the feeder within the specified voltage band, denoted as ΔV_{bnd} . This dispatching problem can be formulated as an optimization problem, where the objective function quantifies the deviation of the node voltages from the ΔV_{bnd} illustrated in Fig. 1. Thus, the objective function can be expressed as follows:

$$f_{j,t}^{\mu} = \sum_{i \in N, i \notin K} (\max(v_{i,j,t} - v^{upper}, 0) + \max(v^{lower} - v_{i,j,t}, 0)), \forall t \in P, \forall t \in T \quad (1)$$

where N represents the set of nodes, K denotes the set of voltage regulators, P is the number of phases, T indicates the scheduling period. $v_{i,j,t}$ is the voltage on phase j at node i at time t . The lower and upper limits (i.e., v^{lower} and v^{upper}) can be set based on voltage variation on the feeder before the DVC is added.

Due to the potential increase in LVR operations caused by PV intermittency and Var injection from the DVC, an additional objective function can be introduced to mitigate excessive LVR operation. This objective function is defined as the sum of tap movements of the LVRs, as shown below:

$$f_{j,t}^{\theta} = \sum_{k \in K} |\theta_{k,j,t} - \theta_{k,j,t-1}|, \forall t \in P, \forall t \in T \quad (2)$$

where $\theta_{k,j,t}$ is the tap position of regulator on phase j at node k at time t .

By incorporating these objective functions, the problem of optimal dispatch can be formulated as follows:

$$\text{minimize}_{Q_{j,t}^{inj}} \quad w_{\mu} f_{j,t}^{\mu} + w_{\theta} f_{j,t}^{\theta} \quad (3)$$

$$\text{s.t.} \quad 0 \leq |Q_{j,t}^{inj}| \leq 1, \forall t \in P, \forall t \in T \quad (4)$$

The first objective function, which aims to reduce voltage variation, is assigned higher weights to emphasize its importance. To solve this problem, an iterative search method is used to determine the optimal Q_{inj} for a given feeder operating condition, considering load and PV levels.

2.2 DVC Dispatch Performance

To assess how much the DVC reduced the voltage variations and limited the voltage regulator operations, four performance metrics are used: lower voltage violations (V_{out}^{lower}), within a target voltage band (V_{in}), upper voltage violations (V_{out}^{upper}), and voltage regulator operations Tap_k .

$$V_{out}^{lower} = \sum_{t \in T_1} t, \quad T_1 = \{t \in T \mid V_t < V^{lower}\} \quad (5)$$

$$V_{in} = \sum_{t \in T_2} t, \quad T_2 = \{t \in T \mid V^{lower} \leq V_t \leq V^{upper}\} \quad (6)$$

$$V_{out}^{upper} = \sum_{t \in T_3} t, \quad T_3 = \{t \in T \mid V^{upper} < V_t\} \quad (7)$$

$$Tap_k = \sum_{t \in T} |\theta_{k,t} - \theta_{k,t-1}|, \quad \forall k \in K \quad (8)$$

2.3 DVC Placement

Since the DVC injects reactive power, it primarily influences the voltages in the zone in which it is placed. To illustrate this, examine the sample feeder depicted in Fig. 2. In this system, the LVR (i.e., 160R) on the main feeder divides the feeder into two distinct voltage zones, as indicated in Fig. 2. Zone 1 represents the first voltage zone (highlighted in orange), while Zone 2 corresponds to the second zone (highlighted in green).

Time-series power flow simulations are first conducted on the feeder with no DVC, which serves as the base case. Figure 3 shows the phase-wise voltage distribution, sorted in descending order based on average voltage. The figure effectively demonstrates the contrasting voltage variations observed in the two zones. Zone 1 exhibits significantly larger voltage variations compared to Zone 2, mainly due to a large PV farm. Furthermore, Zone 1 experiences greater voltage imbalance between phases compared to Zone 2. Consequently, our objective is to examine the effectiveness of the DVC in mitigating voltage variations specifically within Zone 1. Considering that the DVC influences voltages in the vicinity of its placement node, we identified the node with the highest voltage variations within the targeted zone. For the given sample feeder, candidate nodes were selected by evaluating the voltage variation profiles. The dispatching scheme uses a binary search algorithm to determine the appropriate VAR injection/absorption required by the DVC on a per-phase basis. The following straightforward search procedure for candidate nodes determines which node yields optimal DVC performance:

- a) Place the DVC at a candidate node.
- b) Perform time series power flow simulation on the feeder over the sample days. Time resolution is 1 minute. The DVC is dispatched at every time step of the simulation by using the optimal DVC dispatch scheme.
- c) Repeat the process by moving DVC to a new candidate bus.

3. Supervisory Dispatch For DVC

3.1 Optimal Q-V Trajectories

Figure 12 shows the optimal Q-V trajectories obtained by using the proposed optimal dispatch scheme on the sample system. The figure clearly illustrates that these optimal Q-V trajectories can be quite different than the Volt/Var Curve (VV-C) proposed in IEEE Std. 1547-2018 for local control. The standard VV-C as shown in Fig. 4, is a piecewise linear curve with negative slope. When the voltage exceeds an upper limit (i.e., V^{upper}), the DVC absorbs the reactive power to prevent further voltage rise. On the other hand, when the drops below a specific threshold (i.e., V^{lower}), the DVC injects the reactive power to increase the voltage.

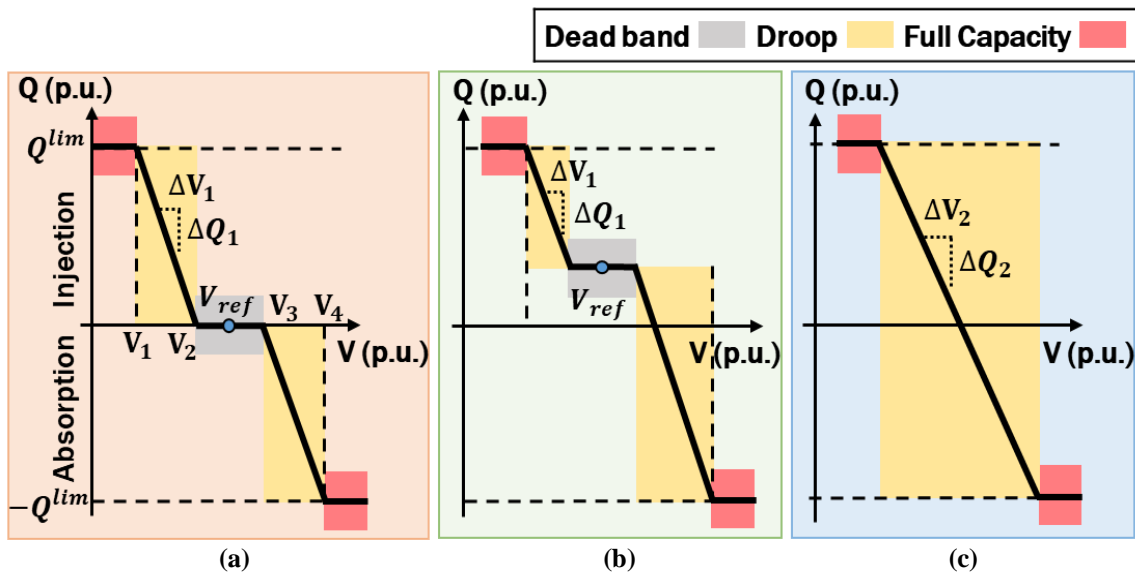


Fig. 4 Volt/Var Curves for (a) Standard (IEEE Std. 1547), (b) Shifted, and (c) Fitted.

3.2 Supervisory Dispatch for DVC

We considered the DVC as a dispatchable Var source and employed an optimization-based dispatching scheme to continuously optimize its performance in terms of minimizing voltage variations. However, this approach faces a significant challenge due to the frequent dispatch signals required, which may not be practical in distribution systems with limited communication infrastructure. To overcome this challenge, a local control scheme, initially proposed for smart inverters and utilizing the VV-C specified in IEEE Std. 1547 (shown in Fig. 4), is currently utilized for the DVC. Nevertheless, to ensure the effectiveness of the DVC using this local control strategy, proper adjustment and setting of the VV-Cs are necessary. The optimal Q-V trajectories presented in the case study clearly illustrate the need for periodic adjustments. To address this issue, we investigated the problem and developed two supervisory control schemes that determine the optimal frequency of VV-C adjustments for the DVC to provide effective voltage support under varying operating conditions. These supervisory schemes monitor the performance of the DVC and make necessary adjustments to the VV-C, periodically sending the revised characteristics to the DVC. The proposed scheme involves two main steps: time segmentation and VV-C curve

fitting based on the optimal Q-V profiles obtained for the respective time segment. The steps are outlined below.

1) *Time Segmentation*: The objective of time segmentation is to identify shorter time segments that allow for a good fit between the Q-V trajectories observed during these segments and the VV-C characteristics. Based on the results obtained from the optimal dispatch, it was observed that the voltage variations on the feeder are considerable during periods of highly variable PV output. Consequently, the Q dispatch of the DVC is adjusted accordingly to mitigate these variations. Conversely, when the PV output is low, the change in Q dispatch is not substantial. Therefore, the time segmentation is determined based on the PV output. In Fig. 5, Segment 1 represents a period of low PV output when the PV generation is less than 25% of the load, while Segment 2 corresponds to a period of high PV output (highlighted in yellow) when the PV generation exceeds 25% of the load. By dividing the time into these distinct segments, we can better align the VV-C characteristics with the observed Q-V trajectories during different PV output conditions.

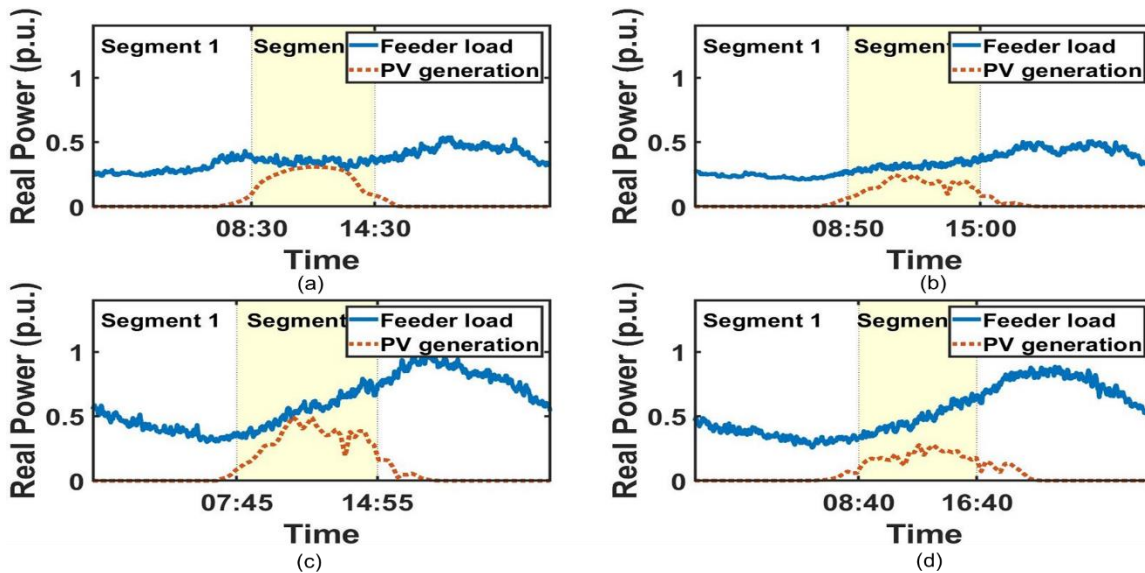


Fig. 5 Time segmentation based on PV output, (a) Winter, (b) Spring, (c) Summer, and (d) Fall.

2) *Volt/Var Curve (VV-C) Fitting*: We propose two schemes for updating the VV-C for the DVC. The first scheme, called *curve shifting*, involves shifting the midpoint of the standard VV-C (i.e., V_{ref}) to align with the average Q-V point obtained from the optimal Q-V trajectory. Only the V_{ref} value is adjusted while maintaining the slope of the existing curve. In the second approach, called *fitted VV-C*, we use linear regression [weisberg2005] applied to determine the slope that best fits the VV-C to closely match the optimal Q-V trajectory.

The next step is to determine the frequency at which the VV-C should be updated to ensure effective voltage support under varying operating conditions. As illustrated in Fig. 5, Segment 1 experiences low PV output, and thus the IEEE Std. 1547 VV-C is adopted. In Segment 2, with significant PV output, the VV-C is updated using the optimal dispatch results obtained for this segment. It is worth noting that the ideal approach would involve utilizing the optimal Q dispatch and voltage for the subsequent interval. Established methods, such as statistical or neural network-

based approaches, can be employed for short-term load and solar PV forecasting to facilitate this process. However, this is not the focus of this paper, therefore the simplest prediction available is to assume that we already know the predictions for the next interval.

3. Case Study

The IEEE 123 node test system shown in Fig. 2 is used to test and demonstrate the effectiveness of the proposed DVC optimal dispatching scheme in unbalanced scenario. To simulate high PV penetration on the feeder, a 5 MW PV farm is placed at node 54 and a 1 MVar 3-phase DVC is considered. OpenDSS is used to do the time series power flow simulations and the DVC is modelled as three single-phase reactor banks with independent control on each phase. The load and PV profiles utilized in this study are obtained from two different data sources. The 1-minute smart meter data sets are sourced from the Pecan Street data repository, while the 1-minute PV data sets are collected from Duke Energy in North Carolina. Figure 6 presents the normalized load and PV profiles for four selected sample days.

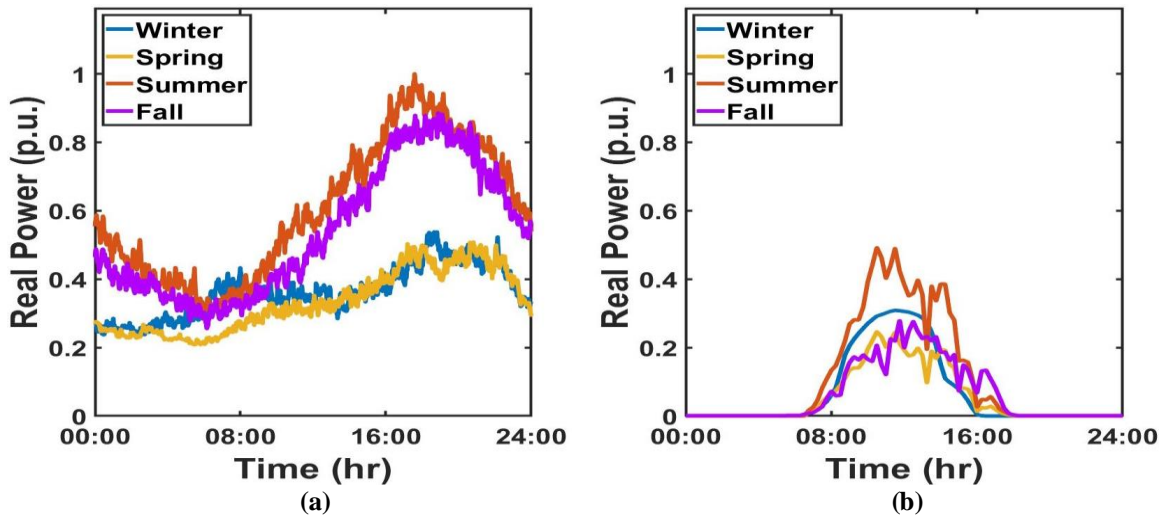


Fig. 6 Real power of (a) Feeder load, (b) PV output.

3.1 DVC Placement

The proposed approach is applied to determine the optimal location for the DVC in the system. Firstly, the node voltage variations in Zone 1, where the DVC is intended to be placed, are obtained without the DVC (i.e., base case). The voltage profiles obtained are depicted in Fig. 3. Based on these profiles, three candidate nodes (i.e., nodes 7, 8, and 13) are selected as they have the largest voltage variations. Subsequently, the DVC is positioned at these candidate locations, and the optimal dispatch is used to evaluate the effectiveness of the DVC in mitigating voltage variations on the feeder. Table 1 presents the performance metrics obtained for these three scenarios. The total voltage points (T) monitored during the scheduling period is 1,578,240.

| Node No. | $V_{lower\ out}$ (1) | V_{in} (2) | $V_{upper\ out}$ (3) | Out of limits (%) ((1)+(3))/(T) |
|----------|-------------------------|-----------------|-------------------------|------------------------------------|
| Base | 3,766 | 1,110,433 | 464,041 | 29.64 |
| 7 | 1,620 | 1,284,277 | 292,343 | 18.63 |
| 8 | 2,624 | 1,330,004 | 245,612 | 15.73 |
| 13 | 5,308 | 1,288,206 | 284,726 | 18.38 |

Table 1. Voltage Violations of 3 Candidate Nodes.

Figure 7 shows the node voltage histograms for the three scenarios, revealing the impact of placing the DVC at these locations on reducing voltage variations among the feeder nodes. The results demonstrate a notable improvement, as a significant portion of node voltages now fall within the desired voltage band. Specifically, the percentage of node voltages outside the band decreases from 29.6% in the base case to 15.7% when the DVC is placed at node 8. Moreover, the voltage variation statistics show slight variations across the different phases of the circuit. Importantly, the performance metrics between the selected nodes show no significant differences, indicating that any of the chosen nodes can be suitable. However, we chose node 8 as the optimal location since it yields the most favorable statistics for both the lower and upper voltage bands.

Figure 8 provides an evaluation of the performance of the DVC by examining voltage variations at three selected nodes (29, 66, and 8) in Zone 1, both with and without the presence of the DVC at node 8. Node 8 represents the location where the DVC is placed, while nodes 29 and 66 are the farthest nodes connected to the mainline within the same zone. As depicted in the Fig. 8, the DVC demonstrates a noticeable reduction in the occurrences of low voltages (< 0.98) and high voltages (> 1.03). However, note that the impact of the DVC on nodes 29 and 66 is minimal, with only slight changes observed. Conversely, the DVC significantly diminishes voltage variations at the node to which it is connected. This observation suggests that the DVC is particularly effective in reducing voltages at the bus it is connected and neighboring buses.

3.2 Optimal Dispatch

The placement of the DVC at node 8 (i.e., Case 1) introduces an undesirable effect, leading to an increase in LTC and LVR operations compared to the base case (i.e., Case 0), as shown in Table 3 and Figure 10. The results highlight a significant increase in tap operations. This issue emphasizes the need for an optimal DVC dispatching approach that considers two objectives: f^μ , the primary objective aimed at minimizing voltage variations, and f^θ , the secondary objective aimed at limiting LVR tap changes. Since the number of tap operations is numerically a large value compared to f^μ , we tried with two different weights for f^θ : 1 and 0.1. To determine the most suitable option among these alternatives, we simulated the following four cases:

- a) **Case 0 (Base Case):** This is the base case which corresponds to the system without the DVC.

- b) **Case 1:** This case only considers the voltage variation (f^μ) as the main objective for the DVC dispatch. The dispatching scheme is employed to determine the appropriate VAR injection/absorption required for the DVC to minimize voltage variations.
- c) **Case 2:** In this case, the objective for the DVC dispatch combines both the voltage variation metric f^μ with $w_\mu = 1$ and tap changes metric f^θ with $w_\theta = 1$.
- d) **Case 3:** This case is the same as Case 2 but the weight for the LVR tap metric f^θ with $w_\theta = 0.1$.

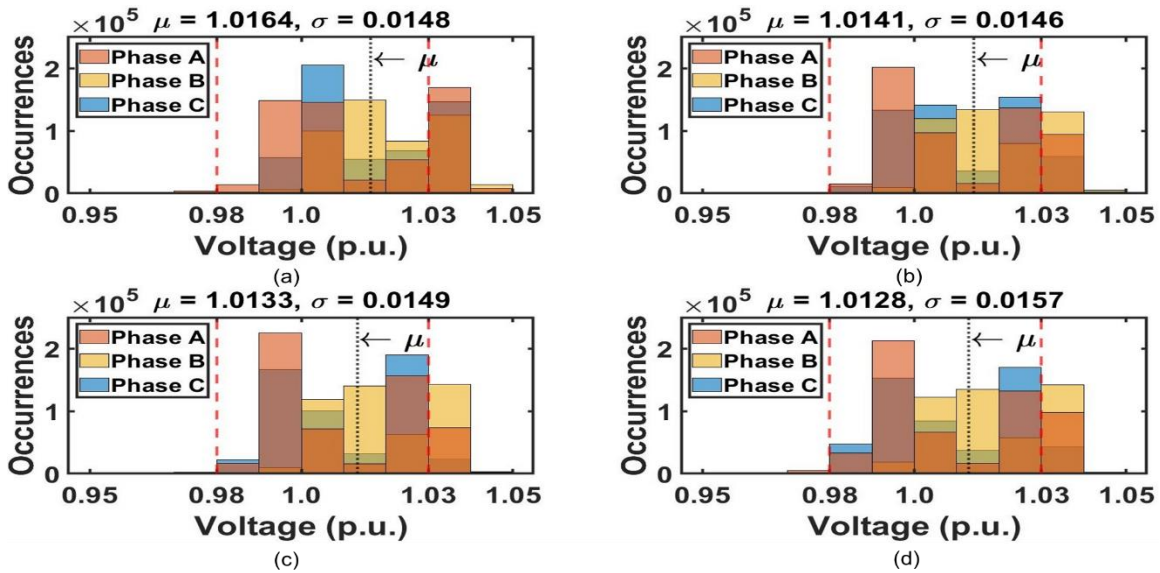


Fig. 7 Voltage distribution by DVC placement, (a) no DVC, (b) node 7, (c) node 8, and (d) node 13.

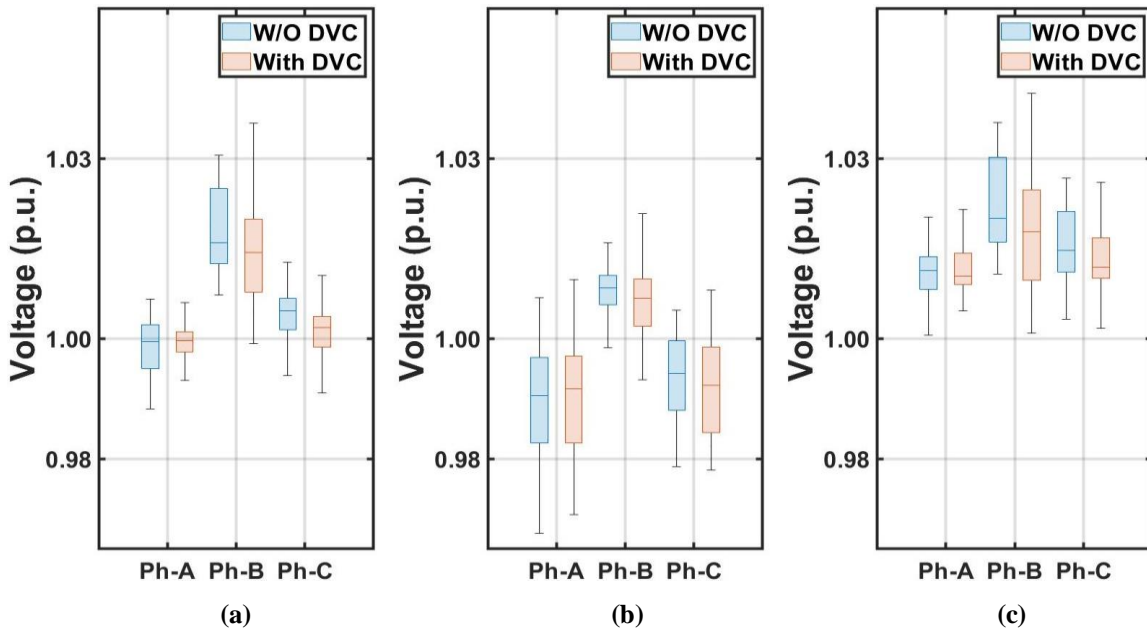


Fig. 8 Distribution of voltage variations with and without DVC (a) at node 29, (b) at node 66, and (c) node 8.

| Case No. | | | | Out of limits (%) |
|----------|-------|-----------|---------|-------------------|
| | (1) | (2) | (3) | $((1)+(3))/(T)$ |
| 0 (Base) | 3,766 | 1,110,433 | 464,041 | 29.64 |
| 1 | 2,624 | 1,330,004 | 245,612 | 15.73 |
| 2 | 3,882 | 1,128,737 | 445,621 | 28.48 |
| 3 | 3,032 | 1,255,760 | 319,448 | 20.43 |

Table 2. Voltage Violations by Case.

| Case No. | LTC | LVR | | | | | | Total |
|----------|------|------|------|------|------|------|------|-------|
| | 3-ph | Ph-A | Ph-A | Ph-C | Ph-A | Ph-B | Ph-C | |
| | 150R | 9R | 25R | 25R | 160R | 160R | 160R | |
| 0 (Base) | 19 | 6 | 107 | 54 | 43 | 32 | 15 | 276 |
| 1 | 160 | 83 | 290 | 908 | 69 | 67 | 625 | 2,202 |
| 2 | 34 | 11 | 48 | 110 | 24 | 26 | 21 | 274 |
| 3 | 28 | 7 | 70 | 180 | 27 | 97 | 129 | 538 |

Table 3. LTC and LVR Tap Changes by Case.

Simulation results for these four cases are summarized in Tables 2 and 3. The key observations are summarized below:

- Compared to Case 0 (base case), Cases 1, 2, and 3 all reduce node voltage variations, as indicated by the performance statistics presented in Table 2. Figure 9 shows the voltage distribution for the four cases, highlighting how the voltages are shifted closer to the desired voltage band.
- Figure 10 compares the number of LTC and LVR operations across different cases. The results demonstrate that focusing only on voltage variation in the dispatch (Case 1) leads to an increase in LVR operations. However, Case 3, which incorporates the revised objective, provides a good compromise by reducing LVR operations compared to Case 1, without degrading the voltage variation performance of the DVC.
- Figure 11 shows the optimal Q dispatch results and voltage at node 8 for each case. The results reveal that the DVC primarily injects reactive power (kVar) throughout the duration. Furthermore, the terminal voltage at node 8 consistently remains in close proximity to the upper voltage band limit of 1.03 pu.

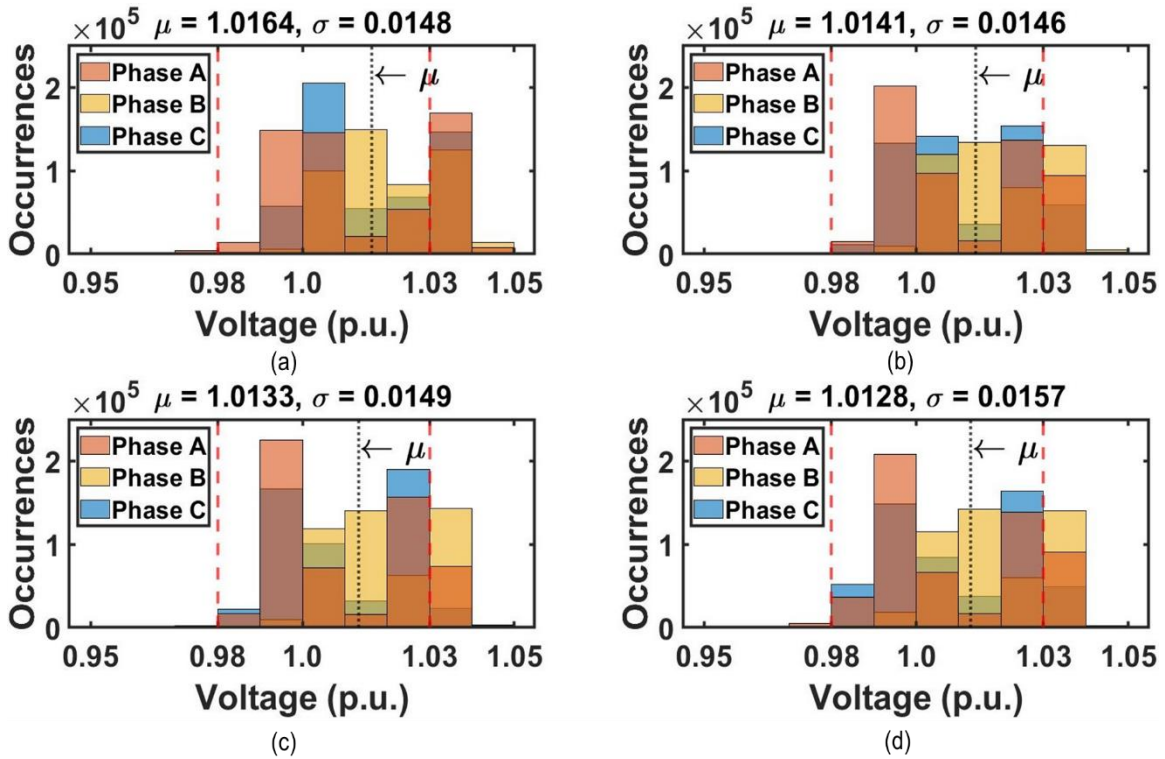


Fig. 9 Voltage distribution by case, (a) Case 0, (b) Case 1, (c) Case 2, and (d) Case 3.

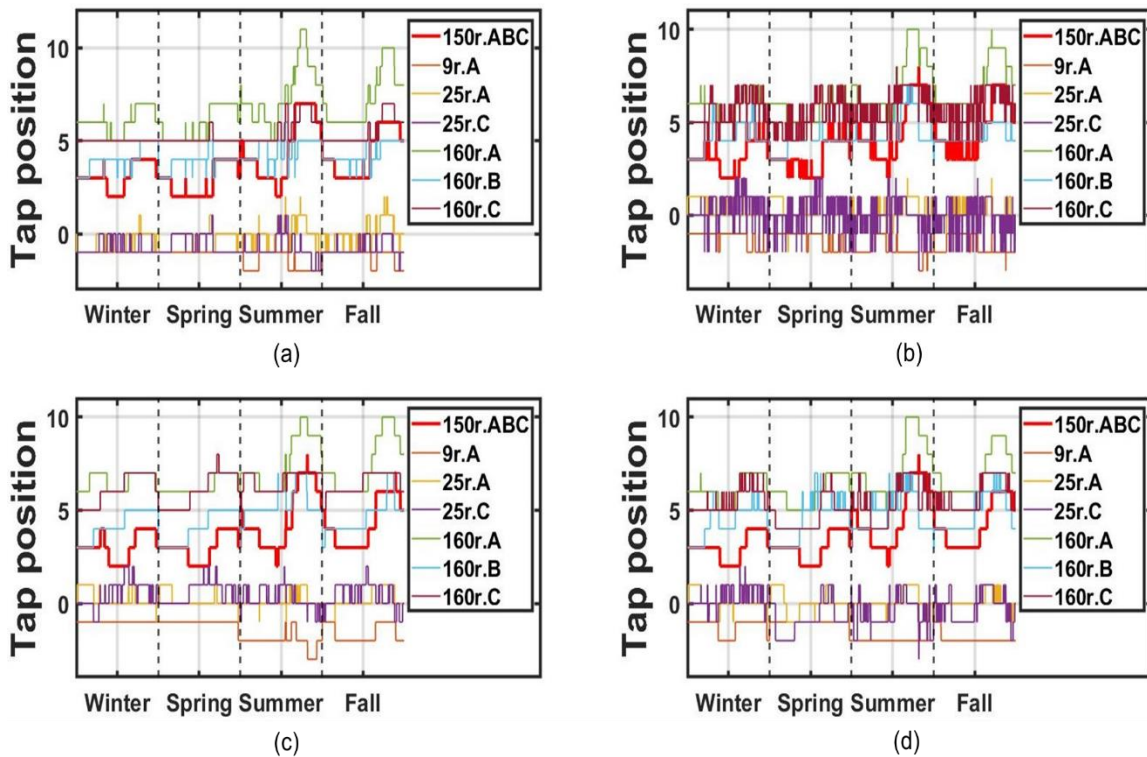


Fig. 10 LTC and LVR tap changes by case, (a) Case 0, (b) Case 1, (c) Case 2, and (d) Case 3.

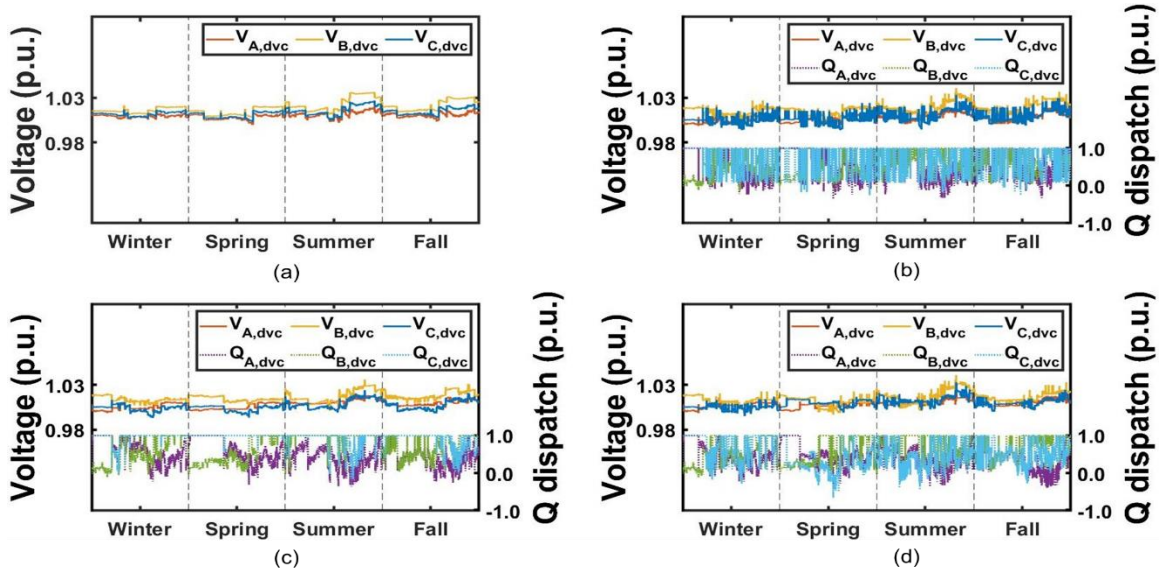


Fig. 11 Voltage and Q dispatch of DVC for (a) Base, (b) Case 1 (c) Case 2, and (d) Case 3.

3.3 Selecting Weights for Dispatch with Combined Objectives

Based on the aforementioned findings, it can be inferred that the voltage variation outcomes are influenced by the weight assigned to tap change metrics. Therefore, a sensitivity analysis is performed to assess the effects of varying tap change weights on the results. The simulations are repeated using different weights of $w_\theta = \{0.01, 0.05, 0.1, 0.5\}$.

The results presented in Tables 4 and 5 demonstrate the importance of adjusting the weight parameter to achieve an optimal compromise solution. It is evident that finding the right balance between reducing voltage variation and limiting the increase in LVR tap operations is crucial. In the case of this system, a weight value of $w_\theta (= 0.05)$ provides a favorable trade-off, effectively minimizing voltage variation while limiting the increase in LVR tap operations.

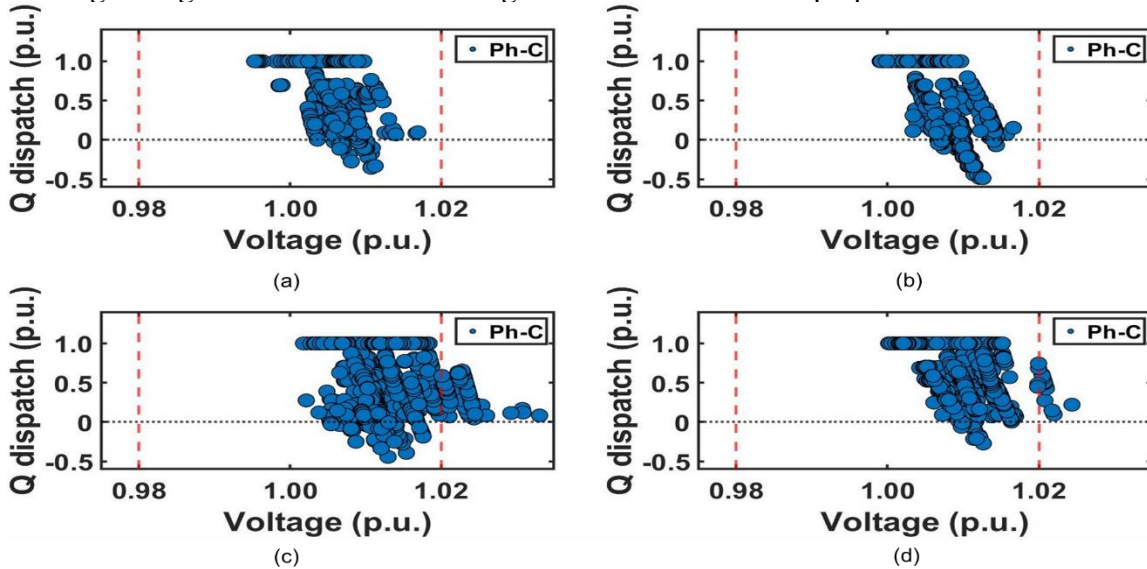


Fig. 12 Optimal Q-V points of Phase C for (a) Winter, (b) Spring, (c) Summer, and (d) Fall.

| W_{θ} | $V_{lower\ out}$ | V_{in} | $V_{upper\ out}$ | Out of limits (%) |
|--------------|------------------|-----------|------------------|-------------------|
| | (1) | (2) | (3) | ((1)+(3))/(T) |
| 0.01 | 4,935 | 1,306,511 | 266,794 | 17.22 |
| 0.05 | 3,032 | 1,268,850 | 306,358 | 19.60 |
| 0.1 | 3,032 | 1,255,760 | 319,448 | 20.43 |
| 0.5 | 3,882 | 1,128,737 | 445,621 | 28.48 |

Table 4. Voltage Violations by Case.

| W_{θ} | LTC | LVR | | | | | | Total |
|--------------|------|------|------|------|------|------|------|-------|
| | 3-ph | Ph-A | Ph-A | Ph-C | Ph-A | Ph-B | Ph-C | |
| | 150R | 9R | 25R | 25R | 160R | 160R | 160R | |
| 0.01 | 80 | 29 | 102 | 298 | 45 | 109 | 171 | 834 |
| 0.05 | 28 | 9 | 72 | 176 | 29 | 97 | 121 | 532 |
| 0.1 | 28 | 7 | 70 | 180 | 27 | 97 | 129 | 538 |
| 0.5 | 34 | 11 | 48 | 110 | 24 | 26 | 21 | 274 |

Table 5. Voltage Violations by Tap Change Weight.

3.4 Supervisory Dispatch

Figure 12 shows the optimal Q-V trajectories without the application of time segmentation. Notably, these trajectories deviate from the standard VV-C, with the optimal Volt-Var points predominantly distributed in a vertical manner rather than horizontally. Thus, many of these points reside within the dead band region of the standard VV-C. To achieve a more accurate fit, we use the proposed time segmentation and focus on Segment 2 as depicted in Fig. 5. This particular segment deserves attention as it corresponds to the time period characterized by large voltage variations.

We proceeded to examine the impact of varying VV-C update frequencies for the DVC. We conducted tests using update rates of 30, 60, 120, and 240 minutes. Figure 13 presents a sample of the optimal Q-V trajectories and the VV-Cs fitted using the two proposed approaches: *curve shifting* and *fitted VV-C*. These particular results focus on the use of 120-minute updates. The findings reveal an enhancement in curve fitting as there is a closer alignment between the adjusted VV-Cs and the optimal Q-V curves. Note that the fitted VV-C exhibits a closer proximity to the optimal Q-V trajectories, primarily because we have the capability to adjust the slope in this case.

We conducted additional simulations on the sample system with the DVC using the revised VV-Cs under local control. Tables 6 and 7 show the statistics for voltage variation and voltage regulator operation for different cases: base case, standard VV-C, shifted VV-C, and fitted VV-C, respectively. These results demonstrate a substantial reduction in voltage variations compared to the standard VV-C when using the revised curves. Comparing these new statistics with those

obtained from optimal dispatch in Table 4, we observe that the improvement in reducing voltage variation is not as significant as with optimal dispatch. However, it is still notably more effective than applying the standard VV-C.

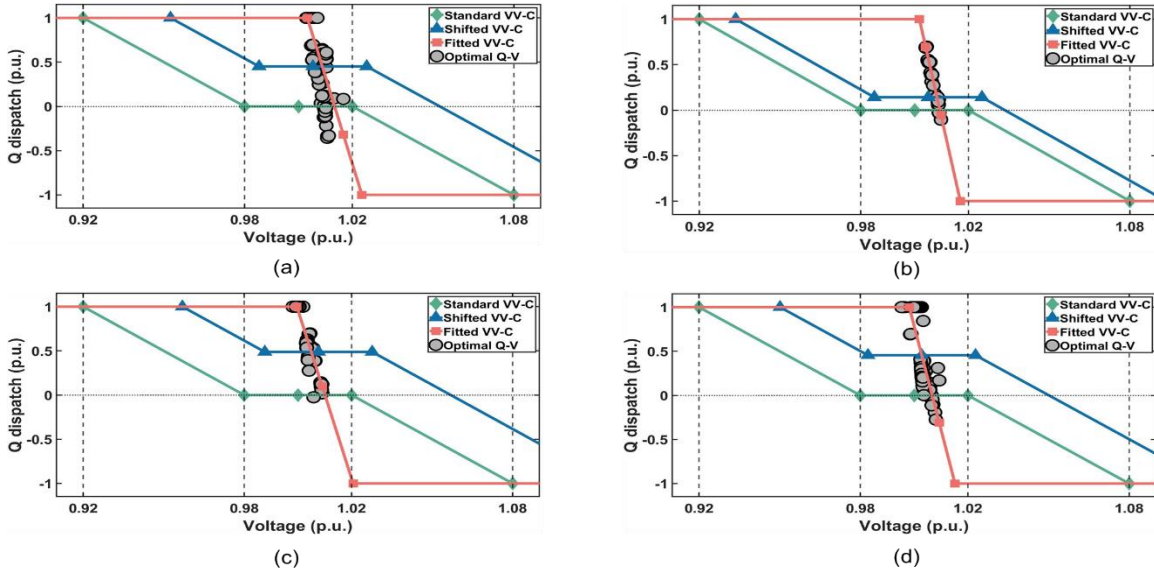


Fig. 13 Optimal Q dispatch of the DVC at Phase C in winter and local control scheme for (a) 08:00-10:00, (b) 10:00-12:00, (c) 12:00-14:00, and (d) 14:00-16:00.

| WC | | (1) | (2) | (3) | Out of limits(%) |
|-----------|---------|-------|-----------|---------|------------------|
| | | | | | $((1)+(3))/(T)$ |
| Base | | 3,766 | 1,110,433 | 464,041 | 29.64 |
| IEEE 1547 | | 3,506 | 1,111,784 | 462,950 | 29.56 |
| Shifted | 30-min | 3,604 | 1,110,343 | 464,293 | 29.65 |
| | 60-min | 3,848 | 1,114,358 | 460,034 | 29.39 |
| | 120-min | 4,652 | 1,124,538 | 449,050 | 28.75 |
| | 240-min | 5,040 | 1,119,536 | 453,664 | 29.06 |
| Fitted | 30-min | 3,369 | 1,103,035 | 471,836 | 30.11 |
| | 60-min | 3,620 | 1,107,966 | 466,654 | 29.80 |
| | 120-min | 4,471 | 1,121,561 | 452,208 | 28.94 |
| | 240-min | 4,591 | 1,120,875 | 452,774 | 28.98 |

Table 6. LTC and LVR Tap Changes by Tap Change Weight.

| VVC | LTC | LVR | | | | | | Total | |
|-----------|---------|------|------|------|------|------|------|-------|-----|
| | 3-ph | Ph-A | Ph-A | Ph-C | Ph-A | Ph-B | Ph-C | | |
| | 150R | 9R | 25R | 25R | 160R | 160R | 160R | | |
| Base | 19 | 6 | 107 | 54 | 43 | 32 | 15 | 276 | |
| IEEE 1547 | 19 | 6 | 101 | 54 | 45 | 31 | 15 | 271 | |
| Shifted | 30-min | 28 | 4 | 94 | 54 | 46 | 47 | 18 | 291 |
| | 60-min | 23 | 4 | 89 | 47 | 43 | 35 | 17 | 258 |
| | 120-min | 18 | 5 | 86 | 42 | 48 | 27 | 13 | 239 |
| | 240-min | 22 | 8 | 79 | 53 | 38 | 24 | 14 | 238 |
| Fitted | 30-min | 32 | 8 | 81 | 44 | 39 | 47 | 15 | 266 |
| | 60-min | 23 | 8 | 85 | 42 | 40 | 34 | 12 | 244 |
| | 120-min | 19 | 4 | 74 | 37 | 38 | 27 | 12 | 211 |
| | 240-min | 20 | 7 | 81 | 40 | 38 | 25 | 13 | 224 |

Table 7. Voltage Violation by Different VVC.

3.5 Sunny vs. Cloudy Days

The impact of PV output variability on voltage variation is more pronounced on cloudy days compared to sunny days. Figure 14 presents the normalized load and PV profiles for both sunny and cloudy days. We examined the effectiveness of the DVC in mitigating high voltage variations caused by cloud cover. For this analysis, we employed a 120-minute update frequency, which demonstrated the best performance according to Tables 6 and 7. The total voltage points (T) monitored on both sunny and cloudy days are 394,560 respectively. The main observations from the simulation analysis can be summarized as follows:

- The DVC shows greater effectiveness in reducing voltage variations on cloudy days compared to sunny days due to its rapid response to PV variability. Table 8 demonstrates the performance of the DVC with fitted VV-C, showing a 3.0% reduction in voltage variations on sunny day and a 3.8% reduction on cloudy day when compared to the base case without DVC.
- The proposed local dispatch schemes, namely the shifted and fitted VV-Cs, outperform the standard VV-C (i.e., IEEE Std. 1547). On sunny day, the shifted VV-C reduced voltage variations by 0.2%, while the fitted VV-C mitigated them by 1.7%. Similarly, on cloudy day, the shifted VV-C reduced voltage variations by 1.7%, while the fitted VV-C achieved a greater reduction of 3.4%.
- The proposed scheme also effectively limits the increase in LVR operations. According to Table 9, the DVC with the fitted VV-C reduces voltage regulator operations from 96 to 87 (9.4% reduction) on sunny days and from 145 to 132 (9.0% reduction) on cloudy days, respectively.

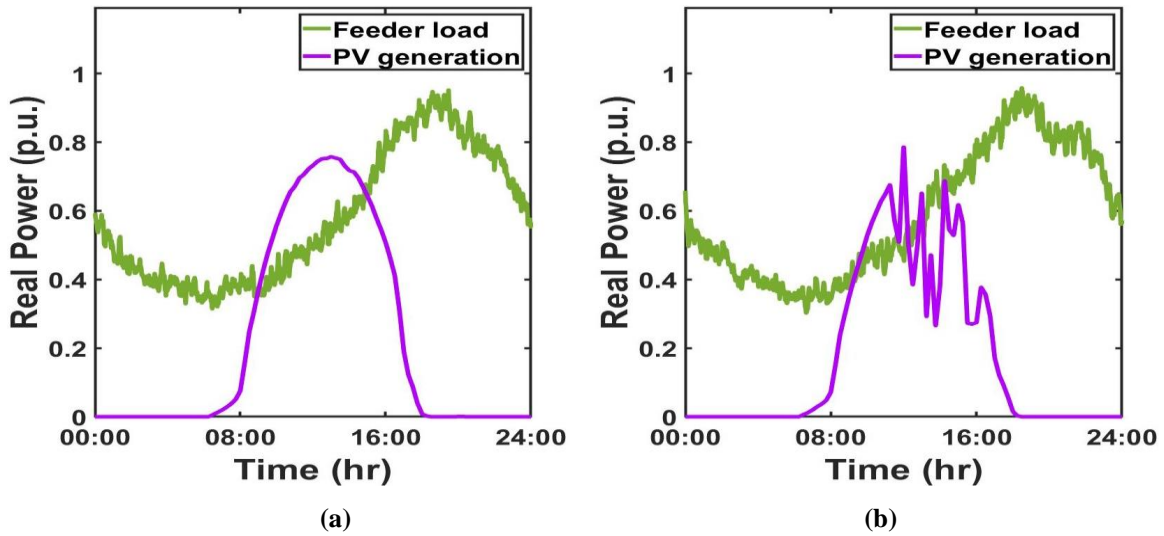


Fig. 14 Real power profile of load and PV for (a) Sunny day, (b) Cloudy day.

| Day | WC | V_{lower}^{out} | V_{in} | V_{upper}^{out} | Out of limits(%) ((1)+(3))/(T) |
|--------|-----------|-------------------|----------|-------------------|-----------------------------------|
| | | (1) | (2) | (3) | |
| Sunny | Base | 1,566 | 268,637 | 124,357 | 31.91 |
| | IEEE 1547 | 1,444 | 270,292 | 122,824 | 31.50 |
| | Shifted | 1,444 | 270,531 | 122,585 | 31.43 |
| | Fitted | 1,444 | 272,413 | 120,703 | 30.96 |
| Cloudy | Base | 1,418 | 271,024 | 122,118 | 31.31 |
| | IEEE 1547 | 1,333 | 271,471 | 121,756 | 31.20 |
| | Shifted | 1,447 | 273,564 | 119,549 | 30.67 |
| | Fitted | 1,353 | 275,703 | 117,504 | 30.12 |

Table 8. LTC and LVR Tap Changes by Different VVC.

| Day | VVC | LTC | | LVR | | | | | Total |
|--------|-----------|--------------|------------|-------------|-------------|--------------|--------------|--------------|-------|
| | | 3-ph 150R | Ph-A 9R | Ph-A 25R | Ph-C 25R | Ph-A 160R | Ph-B 160R | Ph-C 160R | |
| | | | | | | | | | |
| Sunny | Base | 9 | 4 | 42 | 23 | 15 | 9 | 4 | 106 |
| | IEEE 1547 | 9 | 4 | 36 | 24 | 12 | 7 | 4 | 96 |
| | Shifted | 9 | 5 | 29 | 25 | 15 | 7 | 4 | 94 |
| | Fitted | 9 | 5 | 25 | 23 | 12 | 8 | 5 | 87 |
| Cloudy | Base | 14 | 5 | 48 | 37 | 21 | 13 | 6 | 144 |
| | IEEE 1547 | 14 | 5 | 47 | 37 | 22 | 14 | 6 | 145 |
| | Shifted | 14 | 5 | 50 | 34 | 25 | 10 | 9 | 147 |
| | Fitted | 12 | 4 | 38 | 34 | 22 | 13 | 9 | 132 |

Table 9. Voltage Violation on Sunny and Cloudy Days.

4. Conclusion

This research proposes a practical dispatching scheme designed to mitigate the rapid voltage variations caused by PV intermittency on a feeder. The proposed supervisory dispatch scheme adjusts the VV-C utilized by the local DVC controller, overcoming the limitations of existing methods. Through simulations conducted on a sample distribution feeder, the effectiveness of the proposed scheme is demonstrated. The simulations clearly indicate that using standard Volt-Var curves for local DVC control may not effectively reduce voltage variations.

The paper highlights the significance of the proposed approach, which employs a supervisory dispatching scheme to modify these curves, ensuring that the DVC provides efficient voltage variation reduction while minimizing LVR tap operations. Additionally, the paper emphasizes the necessity of an optimal dispatching scheme to properly modify the VV-C. The case study demonstrates the need for adjusting the VV-C about every two hours, particularly during periods of high and variable PV output. Furthermore, the optimal dispatching scheme can be used to determine the optimal DVC placement on a distribution feeder with high PV generation. The case study results illustrate that the proposed heuristics-based scheme is highly effective in determining suitable candidate locations, while maintaining computational efficiency.